COBEM 2021 26th International Congress of Mechanical Engineering
ABCM Associação Brasileira de Engenharia e Ciências Mecânicas
November 22-26, 2021, Virtual Congress, Brazil

COB-2021-1253
PHYSICS INFORMED NEURAL NETWORKS TO IDENTIFY UNBALANCE PARAMETERS IN ROTATING SYSTEM

Lucas Nogueira Garpelli
Helio Fiori de Castro
University of Campinas, R. Mendeleyev, 200, Campinas
l190804@dac.unicamp.br, heliofc@fem.unicamp.br

Abstract. *The improvement of computational resources and a large amount of data produced by different areas of science have made the neural network very relevant among researchers, exploiting their ability to deal with complex problems. However, some applications have difficulty in collecting data for neural network training, either due to the inability to obtain them or the high cost associated with their acquisition. Physics Informed Neural Networks (PINN) use the information from the model that describes the physics behavior of the analyzed system to reduce the need for large amounts of data for network training. In this work, a rotating system was modeled, in order to obtain the dynamic behavior in frequency domain response. These responses and the equation of motion are then used in the PINN to identify the unbalance fault parameters applied to the rotating system.*

Keywords: *Rotordynamics, Unbalance Parameters, Neural Networks, PINN.*

1. INTRODUCTION

Rotating system applications in industry are massive. They are present in the automotive, aerospace, power generation and other industries. The unbalanced force of the rotor mass is an inherent force in rotating systems that can generate excessive vibrations and cause catastrophic failures. Rotor unbalance is a condition of unequal mass distribution in the radial direction that does not coincide with the axis of rotation (Muszynska, 2005).

There are many works published about the rotor unbalance. Muszynska (2005) explores the unbalance response in several rotor systems such as supported by hydrodynamic bearings, anisotropic and isotropic rotor and supports, rubbing contact among others. Some authors focused on identifying unbalance parameters (Vázquez *et al.*, 2001; Lee and Ha, 2005; Gohari and Eydi, 2020), while others investigated diagnosis techniques (Jalan and Mohanty, 2009; Ahamed *et al.*, 2010; Rahman and Uddin, 2017).

Recent researches are using artificial neural network (ANN) to solve unbalance problems. Walker *et al.* (2014) use ANN in subsynchronous nonlinear features in the frequency domain to identified unbalance faults. The authors included rub and misalignment faults in their research and they showed that ANN achieved a high level of accuracy to prediction unbalance faults. Singh and Kumar (2015) compared ANN with support vector machine in unbalanced and misalignment rotors. Both techniques proved fast and reliable detection for rotor faults. Gohari and Kord (2019) simulated a rotary system with four disks and used ANN to identify unbalance force of the rotor. In their study the ANN shows an accuracy between 94 to 96% to quantify the unbalance and its location.

Machine learning has been grown rapidly likewise innovations on this field. Raissi *et al.* (2017a) and Raissi *et al.* (2017b) developed a new class of ANN that use law of physics for its training. Named physics informed neural networks (PINN) this new neural network solves problems using nonlinear partial differential equations (PDEs) in its structure. One of the authors' purposes is to reduce the amount of input data for training. In all benchmarks considered in their work, the total number of training data was relatively small. The researchers showed that even with a reduced amount of data it is possible to obtain good results using PINN. Raissi (2018) kept the previous work and improved using deep learning and nonlinear PDEs from scattered and potentially noisy observations in space and time. Despite the first work with PINN uses PDEs, Misyris *et al.* (2020), Ji *et al.* (2020) and Antonelo *et al.* (2021) demonstrated great results whit ordinary differential equations (ODEs). Some researchers have achieved remarkable results when using PINN in the design of meta-materials, fluid mechanics and chemical kinetics problems (Fang and Zhan, 2020; Sun *et al.*, 2020; Ji *et al.*, 2020). Others authors focused to increase the robustness of PINN and created its variation (Jagtap *et al.*, 2020; Meng *et al.*, 2020; Antonelo *et al.*, 2021; Kharazmi *et al.*, 2021).

In the present work, finite element method (FEM) was used to model a rotor with two disks and the PINN to prediction rotor unbalance parameters like unbalancing mass and unbalance phase between the two disks. This approach advantage is the fast parameters identification, which is an improvement when compared with model-based identification methods that require a significant amount of computational resource.

2. METHODOLOGY

2.1 Rotor machine model

In general rotating machinery is modeling by applying FEM. This is a widespread modeling and has already shown reliable results by several researchers (Archer, 1965; Zorzi and Nelson, 1977; Lalanne and Ferraris, 1998). By applying the FEM each rotor elements are modeled according to its own characteristics. In this study we take into account inertia and gyroscopic effect on the disks but we neglected the flexibility in disk elements. However the inertia, gyroscopic effect and flexibility are considered for the beam elements (Nelson and McVaugh, 1976; Zorzi and Nelson, 1977). The differential equation of motion ig given by

$$\mathbf{M_g}\ddot{\mathbf{q}} + (\mathbf{C_g} + \omega\mathbf{G_g})\,\dot{\mathbf{q}} + \mathbf{K_g}\mathbf{q} = \mathbf{F}, \tag{1}$$

where $\mathbf{M_g}$, $\mathbf{C_g}$, $\mathbf{G_g}$ and $\mathbf{K_g}$ are the mass, damping, gyroscopic and stiffness matrices, respectively, ω is the shaft rotational speed and the subscript g indicates the global matrix of the system; $\mathbf{q} = \{y_1, z_1, \varphi_{y1}, \varphi_{z1}, ..., y_n, z_n, \varphi_{yn}, \varphi_{zn}\}$ are te generalized coordinates of the system which consider all degrees of freedom and the displacement of the rotor in n finite-element discretization nodes; $\mathbf{F} = \mathbf{m}\mathbf{e}\omega^2 - \mathbf{W}$ where $\mathbf{me}$ is the product between unbalance mass and its eccentricity, ω is the shaft rotational speed and $\mathbf{W}$ is the rotor weight. The force is applied just in the degrees of freedom of the disks and is null for the others. The global matrices of damping $\mathbf{C_g}$ and stiffness $\mathbf{K_g}$ take in to account the damping $\mathbf{C_b}$ and the stiffness $\mathbf{K_b}$ matrices of the oil film in the journal bearing,

$$\mathbf{C_b} = \begin{bmatrix} c_{xx} & c_{xy} \\ c_{yx} & c_{yy} \end{bmatrix}, \tag{2}$$

$$\mathbf{K_b} = \begin{bmatrix} k_{xx} & k_{xy} \\ k_{yx} & k_{yy} \end{bmatrix}. \tag{3}$$

A short journal bearing was considered to modeling $\mathbf{C_b}$ and $\mathbf{K_b}$, in this case the ratio between the bearing length l and diameter d has to be less than or equal 0.5 (Ocvirk, 1952; Lund and Sternlicht, 1962; Krämer, 1993). The scheme of a hydrodynamic bearing is shown in Fig. 1. Due to the fact that the shaft is subjected to some load, the bearing center O_b and the shaft center O_s are not coincident. This behavior leads to a journal eccentricity e_j and an attitude angle α, which is the angle from y axis to $\overline{O_bO_s}$. If we define $0 \geq \theta \geq \pi$ along the $\overline{O_bO_s}$, the minimum distance of the shaft from the bearing is obtained by

$$h(\theta) = h_o + e_j \cos(\theta), \tag{4}$$

where h_o represents the bearing clearance.

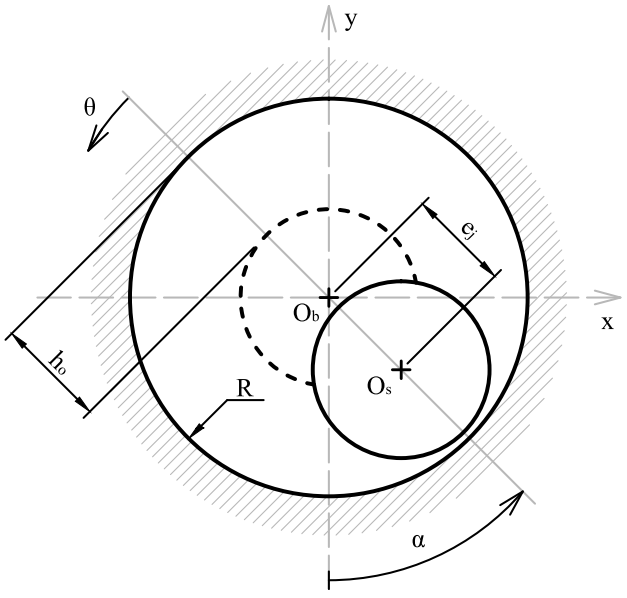

Figure 1. Scheme of journal bearing. Adapted from Krämer (1993)

According with Krämer (1993), the *Reynolds' Equation* for short bearings is given by

$$\frac{1}{R^2}\frac{\partial}{\partial\theta}\left(h^3\frac{\partial p}{\partial\theta}\right)+h^3\frac{\partial^2 p}{\partial z^2}=6\eta\left[\omega\frac{\partial h_o}{\partial\theta}+e_j(\omega-2\dot{\alpha})\sin(\theta)-2\dot{e}_j\cos(\theta)\right], \tag{5}$$

here R represents the bearing radius, p is the oil film pressure and η is the oil viscosity.

According to Ocvirk (1952) and Krämer (1993), by assuming short journal bearing the pressure gradient on the circumferential direction can be considered null ($\partial p/\partial\theta=0$) in comparison to the gradient pressure on the axial direction z. In the case of $z=0$, $\partial p/\partial z=0$ and for $z=\pm l/2$, $p=0$, therefor the analytical expression for the oil film pressure is

$$p(\theta,z,t)=\frac{3\eta}{h^3}[e_j(\omega-2\dot{\alpha})\sin(\theta)-2\dot{e}_j\cos(\theta)]\left(z^2-\frac{l^2}{4}\right). \tag{6}$$

Krämer (1993) demonstrated that by integration over z axis, from $-l/2$ to $l/2$, gives the oil film force per unit length in the circumferential direction. The horizontal and vertical forces on the shaft are calculated by integrating the oil film force over circumferential direction θ, from 0 to π (development of these equations are described by Ocvirk (1952) and Krämer (1993)),

$$F_x=F_\eta f_x(\epsilon,\dot{\epsilon},\dot{\alpha})\cos(\alpha)-\ F_\eta f_y(\epsilon,\dot{\epsilon},\dot{\alpha})\sin(\alpha), \tag{7}$$

$$F_y=F_\eta f_y(\epsilon,\dot{\epsilon},\dot{\alpha})\cos(\alpha)+\ F_\eta f_x(\epsilon,\dot{\epsilon},\dot{\alpha})\sin(\alpha), \tag{8}$$

in which

$$\epsilon=\frac{e_j}{h_o}, \tag{9}$$

$$F_\eta=\frac{\eta l^3\omega R}{2h_o}, \tag{10}$$

$$f_x(\epsilon,\dot{\epsilon},\dot{\alpha})=\ \left(1-\frac{2\dot{\alpha}}{\omega}\right)\frac{2\epsilon^2}{(1-\epsilon^2)^2}+\ \pi\frac{\dot{\epsilon}}{\omega}\frac{1+2\dot{\epsilon^2}}{(1-\epsilon^2)^{5/2}}, \tag{11}$$

and

$$f_y(\epsilon,\dot{\epsilon},\dot{\alpha})=-\frac{\pi}{2}\ \left(1-\frac{2\dot{\alpha}}{\omega}\right)\frac{\epsilon}{(1-\epsilon^2)^{3/2}}-\ \frac{\dot{\epsilon}}{\omega}\frac{4\epsilon}{(1-\epsilon^2)^2}. \tag{12}$$

In the case of a horizontal rotor Eq. 7 is zero and Eq. 8 is the vertical static force on the bearing $-F_o$.

The stiffness and damping coefficients of the oil film are obtained by differentiating the forces F_x and F_y by displacements and velocities at x and y axis, thus

$$k_{xx}=\frac{\partial F_x}{\partial x},\quad k_{xy}=\frac{\partial F_x}{\partial y},\quad k_{yx}=\frac{\partial F_y}{\partial x},\quad k_{yy}=\frac{\partial F_y}{\partial y}, \tag{13}$$

and

$$c_{xx}=\frac{\partial F_x}{\partial \dot{x}},\quad c_{xy}=\frac{\partial F_x}{\partial \dot{y}},\quad c_{yx}=\frac{\partial F_y}{\partial \dot{x}},\quad c_{yy}=\frac{\partial F_y}{\partial \dot{y}}. \tag{14}$$

2.2 Physics informed neural networks

Neural networks are universal function approximators and between their input and output matrices of weights $\mathbf{w}$ and biases $\mathbf{b}$ is applied, the size of these matrices depends on the arrangement of the inputs, outputs and hidden layers in the neural networks. The training process of a neural networks consists of optimizing weights and bias to minimize a loss function. According to Raissi *et al.* (2017a) and Raissi *et al.* (2017b), physics informed neural networks (PINNs) are a class of neural networks constructed to incorporate any law of physics. In its structure the loss function receives the residual values of a mathematical model as a constraint to guarantee that the neural network output satisfies the mathematical model. In a conventional neural networks to achieve good results, a large volume of input data is required. However the PINNs showed good results with reduced amounts of training data.

A wide range of physical problems can be described by parameterized and nonlinear partial differential equations which in general form

$$\frac{\partial u}{\partial t}=-\mathcal{N}[u;\lambda],\quad x\in\Psi,\ t\in[0,T], \tag{15}$$

where $u(t,x)$ represent the underlying solution, $\mathcal{N}[\cdot;\lambda]$ is a nonlinear operator parametrized by λ, and Ψ is a subset of $\mathbb{R}^D$. To impose the physical laws we define the physics informed neural network as

$$f(t,x) = \frac{\partial u}{\partial t} + \mathcal{N}[u;\lambda]. \tag{16}$$

The nonlinear operator $\mathcal{N}[u;\lambda]$ can be simplified to $\mathcal{N}[u]$ if the parameter λ are known. To determine the physics informed neural network $f(t,x)$ it is necessary proceed by approximating $u(t;x)$ by a neural network. As a result the $f(t,x)$ will have the same parameters as $u(t,x)$ and these parameters will be optimized by minimizing the loss function

$$MSE = MSE_u + MSE_f, \tag{17}$$

in which

$$MSE_u = \frac{1}{N_u}\sum_{N_u}^{i=1} |u(t_u^i, x_u^i) - u^i|^2, \tag{18}$$

and

$$MSE_f = \frac{1}{N_f}\sum_{N_f}^{i=1} |f(t_u^i, x_u^i)|^2, \tag{19}$$

where MSE represents the mean squared error loss. The loss MSE_u corresponds to the training data on $u(t;x)$ while MSE_f enforces the law of physics by Eq. 16. N_u is the training data and N_f is the collocation points.

2.3 Physics informed neural networks for rotating system

In Section 2.1 we present the general form of differential equation of motion Eq. 1 in the time domain. This equation generates a large set of displacement data. Therefore, for a wide range of unbalanced mass, this equation would take a lot of computational time to generate all the data needed for training the neural network. Nevertheless, the Eq. 1 can be manipulated to operate in the frequency domain

$$[-\omega^2\mathbf{M_g} + \omega(\mathbf{C_g} + \omega\mathbf{G_g})j + \mathbf{K_g}]\mathbf{Q} = \mathbf{F}e^{\phi}, \tag{20}$$

where ϕ denotes the phase angle. In this new equation of motion the displacement $\mathbf{Q}$ and force $\mathbf{F}$ can be represented by a set of complex conjugated values. In this way the amount of training data in a neural network is dramatically reduced. With the Equation 20 we can define physics-informed neural network as in Eq. 16:

$$f(\mathbf{Q},\mathbf{F}) = [-\omega^2\mathbf{M_g} + \omega(\mathbf{C_g} + \omega\mathbf{G_g})j + \mathbf{K_g}]\mathbf{Q} - \mathbf{F}e^{\phi}, \tag{21}$$

and proceed by approximating the displacements $\mathbf{Q}$ and force $\mathbf{F}$ by a neural network according Eq. 18,

$$MSE_Q = \frac{1}{N_Q}\sum_{N_Q}^{i=1} |Q(y_n^i, z_n^i, \varphi_{yn}^i, \varphi_{zn}^i) - Q^i|^2 + \frac{1}{N_Q}\sum_{N_Q}^{i=1} |F(f_{yn}^i, f_{zn}^i, f_{\varphi yn}^i, f_{\varphi zn}^i) - F^i|^2, \tag{22}$$

where n represent each single node of FEM and N_Q is the number of training data. The Equation 23 is used to enforce the structure imposed by Eq. 21,

$$MSE_f = \frac{1}{N_f}\sum_{N_f}^{i=1} |f(\mathbf{Q}^i, \mathbf{F}^i)|^2, \tag{23}$$

in that N_f is a finite set of collocation points. In this case, the loss function is calculated by $MSE = MSE_Q + MSE_f$.

The rotating system was modeled by FEM with 4 nodes where 2 of then are for the disks that contain the unbalance forces and the other 2 are for the journal bearings (Figure 2). The length between the nodes is $L = 0.30\ m$, the both discs have the same diameter $d_1 = d_2 = 0.08\ m$ and thickness $e_1 = e_2 = 0.02\ m$ and the shaft diameter is $0.015\ m$.

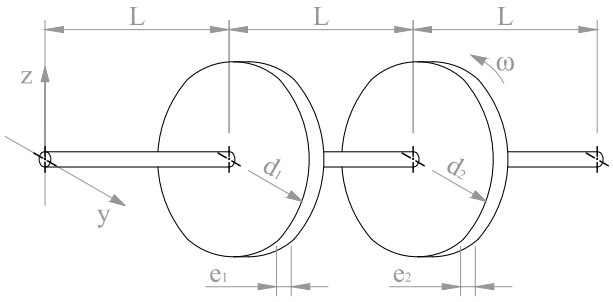

Figure 2. Scheme of rotating system considered for the analysis.

The unbalance moment $\mathbf{me}$ are in range $[1 \times 10^{-5},\ 1 \times 10^{-4}]\ kg.m$ resulting in 5 unbalance moments for each disk. The phase angle ϕ varies within $[-\pi,\ \pi]\ rads$ with a angle step of $\frac{pi}{6}$, resulting in 13 phase angle for each disk. The rotation speed ω is constant and its value is 20 rad/s. As a result, the entire data-set consists of $4,225$ samples for each degree of freedom of the FEM nodes.

3. SIMULATIONS AND RESULTS

In the field, data is usually extracted from the rotor bearings due to the difficulty of measuring at other points of the rotor. For this reason the input data for neural network training are the displacement Q of the journal bearings in the y and z axis. In this case we have 4 inputs and the neural network returns the response of all degrees of freedom of Q and F. As the result we can calculate the unbalance moment by isolating me in $F = me\omega^2 e^{\phi}$ and extract the absolute error between real and calculated unbalance force. For all analyses, we use absolute error because it shows the difference between real and calculated values for all simulated rotors. The absolute error returns its values in percentage and can be calculated using the general form $(|x_{real} - x_{calculated}|/x_{real}) \times 100$.

For all degrees of freedom, we have a set of $4,225$ simulated data and we use $N_Q = 200$ for the training data and $N_f = 3000$ for collocation points. Both training data and collocation points are extracted randomly from the simulated data. After several investigations, we determined the parameters of the neural network that presented good results for the calculation of the unbalance forces. We use 1 hidden layer with 10 neutrons and Rectified Linear Unit (ReLU) as activation function. The training and testing neural networks was performed using TensorFlow in Python.

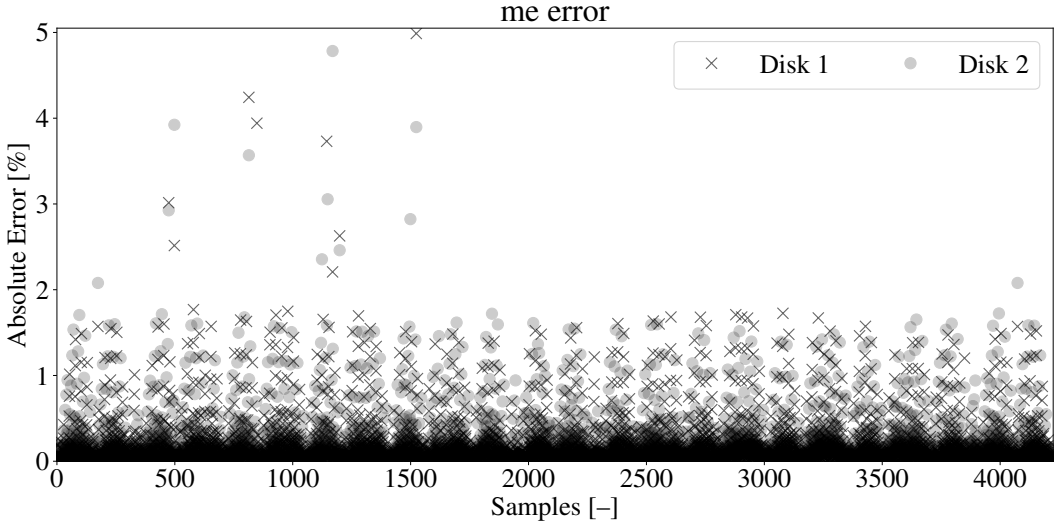

Figure 3. Unbalance moment error for all samples.

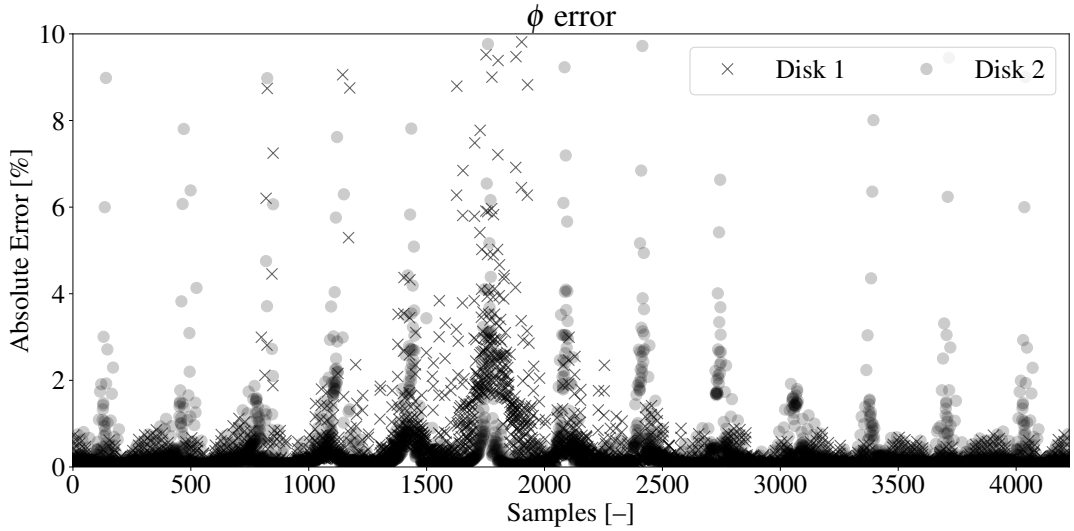

Figure 4. Unbalance phase error for all samples.

Table 1. Mean error in percentage between the predicted and the exact solution of unbalance moment me for different number of training data N_Q and collocation points N_f.

N_Q \ N_f	1000		3000		5000	
	disk1	disk2	disk1	disk2	disk1	disk2
100	0.7516	0.7282	0.3778	0.3751	0.2838	0.2899
200	0.3059	0.3214	0.2499	0.2903	0.2588	0.2336
300	0.3047	0.3132	0.2926	0.2728	0.3019	0.2917
400	0.2175	0.2153	0.2002	0.2081	0.1997	0.1996

Table 2. Mean error in percentage between the predicted and the exact solution of unbalance phase ϕ for different number of training data N_Q and collocation points N_f.

N_Q \ N_f	1000		3000		5000	
	disk1	disk2	disk1	disk2	disk1	disk2
100	0.8793	0.8563	0.4189	0.4923	0.5321	0.4033
200	0.4564	0.4971	0.4032	0.4527	0.3977	0.4038
300	0.4216	0.4848	0.4341	0.4401	0.4171	0.4147
400	0.4122	0.4281	0.3879	0.3801	0.3821	0.3786

The Figure 3 show the absolute error for unbalance mass while Fig. 4 show the absolute error for unbalance phase on the two disks for all simulated examples. In both figures, some samples have an error a little greater than 1% but the vast majority of errors are below 1%. The Table 1 and Table 2 report the mean error in percentage of all simulated data. In these tables, we analyze how the mean error varies when we vary the numbers of training data N_q and collocation points N_f. The results show that when we increase the amount of neural network training data, the average errors decrease.

4. CONCLUSIONS

In this work we analyze how PINN can predict rotor unbalance problems. For this, a rotor with two disks was simulated in which we used different values of the unbalanced mass and phase angle between the two disks. Neural network training was performed with just a few samples of all our data and after training we tested the neural network prediction with all samples. It was possible to notice for a small amount of samples the neural network does not return satisfactory results, however most of the errors remain smaller than 1%. Our results demonstrate the potential for the application of PINN in rotor unbalance problems. Future works will focus on validating analytical results with a real system.

5. ACKNOWLEDGEMENTS

The authors would like to thank CAPES and Petrobras Brazil for providing financial support to this research.

6. REFERENCES

Ahamed, S.K., Karmakar, S., Mitra, M. and Sengupta, S., 2010. "Novel diagnosis technique of mass unbalance in rotor of induction motor by the analysis of motor starting current at no load through wavelet transform". In *International Conference on Electrical Computer Engineering (ICECE 2010)*. IEEE, pp. 474–477. ISBN 1424462800.

Antonelo, E.A., Camponogara, E., Seman, L.O., de Souza, E.R., Jordanou, J.P. and Hubner, J.F., 2021. "Physics-Informed Neural Nets-based Control".

Archer, J.S., 1965. "Consistent matrix formulations for structural analysis using finite-element techniques". *AIAA Journal*, pp. 161–178. ISSN 00011452. doi:10.2514/3.3279.

Fang, Z. and Zhan, J., 2020. "Deep Physical Informed Neural Networks for Metamaterial Design". *IEEE Access*, Vol. 8, pp. 24506–24513. ISSN 21693536. doi:10.1109/ACCESS.2019.2963375.

Gohari, M. and Eydi, A.M., 2020. "Modelling of shaft unbalance: Modelling a multi discs rotor using K-Nearest Neighbor and Decision Tree Algorithms". *Measurement: Journal of the International Measurement Confederation*, Vol. 151. ISSN 02632241. doi:10.1016/j.measurement.2019.107253.

Gohari, M. and Kord, A., 2019. "Unbalance Rotor Parameters Detection Based on Artificial Neural Network". *International Journal of Acoustics and Vibration*, Vol. 24, No. 1, pp. 113–118. ISSN 1027-5851. doi: 10.20855/ijav.2019.24.11272.

Jagtap, A.D., Kawaguchi, K. and Karniadakis, G.E., 2020. "Adaptive activation functions accelerate convergence in deep and physics-informed neural networks". *Journal of Computational Physics*, Vol. 404. ISSN 10902716. doi: 10.1016/j.jcp.2019.109136.

Jalan, A.K. and Mohanty, A.R., 2009. "Model based fault diagnosis of a rotor–bearing system for misalignment and unbalance under steady-state condition". *Journal of Sound and Vibration*, Vol. 327, No. 3, pp. 604–622. ISSN 0022-460X. doi:10.1016/j.jsv.2009.07.014.

Ji, W., Qiu, W., Shi, Z., Pan, S. and Deng, S., 2020. "Stiff-PINN: Physics-informed neural network for stiff chemical kinetics".

Kharazmi, E., Zhang, Z. and Karniadakis, G.E., 2021. "hp-VPINNs: Variational physics-informed neural networks with domain decomposition". *Computer Methods in Applied Mechanics and Engineering*, Vol. 374. ISSN 00457825. doi:10.1016/j.cma.2020.113547.

Krämer, E., 1993. *Dynamics of rotors and foundations*. Springer-Verlag, Berlin, 1st edition. ISBN 3662027984.

Lalanne, M. and Ferraris, G., 1998. *Rotordynamics prediction in engineering*. Wiley, 2nd edition. ISBN 0471972886.

Lee, A.S. and Ha, J.W., 2005. "Prediction of maximum unbalance responses of a gear-coupled two-shaft rotor-bearing system". *Journal of Sound and Vibration*, Vol. 283, pp. 507–523. ISSN 0022460X. doi:10.1016/j.jsv.2004.04.037.

Lund, J.W. and Sternlicht, B., 1962. "Rotor-bearing dynamics with emphasis on attenuation". *Journal of Fluids Engineering, Transactions of the ASME*, pp. 491–502. ISSN 1528901X. doi:10.1115/1.3658688.

Meng, X., Li, Z., Zhang, D. and Karniadakis, G.E., 2020. "PPINN: Parareal physics-informed neural network for time-dependent PDEs". *Computer Methods in Applied Mechanics and Engineering*, Vol. 370. ISSN 00457825. doi: 10.1016/j.cma.2020.113250.

Misyris, G.S., Venzke, A. and Chatzivasileiadis, S., 2020. "Physics-informed neural networks for power systems". In *IEEE Power and Energy Society General Meeting*. pp. 1–5. ISBN 9781728155081. ISSN 19449933. doi: 10.1109/PESGM41954.2020.9282004.

Muszynska, A., 2005. *Rotordynamics*. CRC press. ISBN 1420027794.

Nelson, H.D. and McVaugh, J.M., 1976. "The dynamics of rotor-bearing systems using finite elements". *Journal of Manufacturing Science and Engineering, Transactions of the ASME*, pp. 593–600. ISSN 15288935. doi:10.1115/1.3438942.

Ocvirk, F.W., 1952. "Short-Bearing Approximation for Full Journal Bearings". *National Advisory Committee for Aeronautics*.

Rahman, M.M. and Uddin, M.N., 2017. "Online unbalanced rotor fault detection of an IM drive based on both time and frequency domain analyses". *IEEE Transactions on Industry Applications*, Vol. 53, No. 4, pp. 4087–4096. ISSN 0093-9994. doi:10.1109/TIA.2017.2691736.

Raissi, M., 2018. "Deep Hidden Physics Models: Deep Learning of Nonlinear Partial Differential Equations". *Journal of Machine Learning Research*, Vol. 19, pp. 932–955.

Raissi, M., Perdikaris, P. and Karniadakis, G.E., 2017a. "Physics informed deep learning (Part I): Data-driven solutions of nonlinear partial differential equations".

Raissi, M., Perdikaris, P. and Karniadakis, G.E., 2017b. "Physics informed deep learning (Part II): Data-driven discovery of nonlinear partial differential equations".

Singh, S. and Kumar, N., 2015. "Rotor faults diagnosis using artificial neural networks and support vector machines". *International Journal of Acoustics and Vibrations*, Vol. 20, pp. 153–159. ISSN 10275851. doi: 10.20855/ijav.2015.20.3379.

Sun, L., Gao, H., Pan, S. and Wang, J.X., 2020. "Surrogate modeling for fluid flows based on physics-constrained

deep learning without simulation data". *Computer Methods in Applied Mechanics and Engineering*, Vol. 361. ISSN 00457825. doi:10.1016/j.cma.2019.112732.

Vázquez, J.A., Barrett, L.E. and Flack, R.D., 2001. "A flexible rotor on flexible bearing supports: Stability and unbalance response". *Journal of Vibration and Acoustics, Transactions of the ASME*, Vol. 123, pp. 137–144. ISSN 15288927. doi:10.1115/1.1355244.

Walker, R.B., Vayanat, R., Perinpanayagam, S. and Jennions, I.K., 2014. "Unbalance localization through machine nonlinearities using an artificial neural network approach". *Mechanism and Machine Theory*, Vol. 75, pp. 54–66. ISSN 0094114X. doi:10.1016/j.mechmachtheory.2014.01.006.

Zorzi, E.S. and Nelson, H.D., 1977. "Finite element simulation of rotor-bearing systems with internal damping". *Journal of Engineering for Gas Turbines and Power*, pp. 71–76. ISSN 15288919. doi:10.1115/1.3446254.

7. RESPONSIBILITY NOTICE

The authors are solely responsible for the printed material included in this paper.